Stress Intensity Factor Variations Along Crack Fronts under Three Modes in a Round Bar

Jean Royer, Anh Le Van

Stress Intensity Factor Variations Along Crack Fronts under Three Modes in a Round Bar

J. ROYER and A. Le VAN
Laboratoire de Mécanique des Structures,
Ecole Centrale de Nantes,
1, rue de la Noë, Nantes 44072 Cedex, France

ABSTRACT

Stress intensity factors K_I, K_{II}, K_{III} are given for circular-fronted cracks in a round bar under tensile loading, bending and torsion. These factors are expressed in terms of the crack geometrical parameters and the abcissa on the crack front. The results will allow one to predict the mechanical behaviour of the crack subject to combined loads.

KEYWORDS

Surface crack, circular crack, stress intensity factor, combined modes I+II+III, integral equation method, finite elements.

INTRODUCTION

Conventional experiments carried out on a round bar containing a surface crack in its median section show that the crack front is approximately circular or elliptical. This is why several experimental studies have been conducted on these types of cracks (Bush, 1976, 1981; Astiz et al., 1981, 1986b; Athanassiadis et al., 1981; Salah el din et al., 1981; Nezu et al., 1982; Forman et al., 1984; Underwood et al., 1989).
On the other hand, a lot of numerical works have been devoted to the same crack geometries (Blackburn, 1976; Daoud et al., 1978; Astiz et al., 1980, 1986a,b; Salah el din et al., 1981, 1984; Athanassiadis et al., 1981; Fan et al., 1982; Raju et al., 1984; Caspers et al., 1987). The results are mainly concerned with mode I and a couple of points on the crack front. This paper deals with the numerical problem of circular-fronted cracks in round bars under three modes and the results involve the whole crack front.

DESCRIPTION OF THE PROBLEM

Geometry. Let us consider a round bar of radius R containing a circular-fronted crack in its median section (Fig.1a). Given the crack depth a, the geometries herein considered are located between two bound geometries (Fig.1 b) :
. the so-called semi-circular crack whose radius is equal to a,
. and the so-called straight-fronted crack whose radius tends to infinity.
The front of an intermediate circular crack between the above two geometries intersects the lateral surface of the bar at two points referred to as surface terminal points and denoted by B and B' (Fig.1a), the former lying between B_0 and B_1 (Fig.1 b). It can be easily seen that the

crack geometry is completely defined by the following two dimensionless parameters : the relative crack depth a/R and the shape factor $\alpha \equiv B_0B/B_0B_1 \in [0,1]$ (So $\alpha=0$ corresponds to the semi-circular crack and $\alpha=1$ to the straight-fronted one).

Between the bounds corresponding to $\alpha=0$ and 1, two other geometries are considered, which are defined respectively by $\alpha=1/3$ and $2/3$, thus dividing the arc B_0B_1 into three equal sub-arcs (Fig.1c).

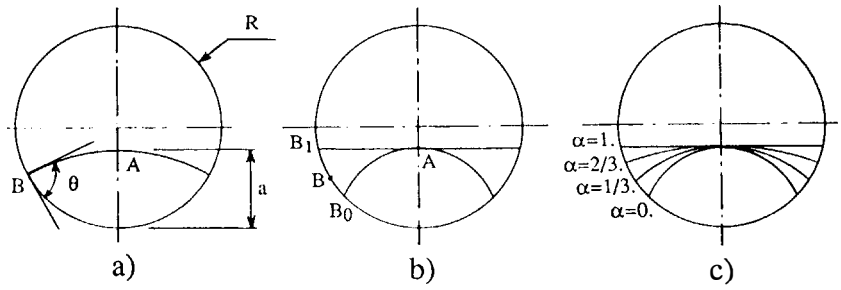

Fig. 1. Geometry of the crack

Six relative crack depths are computed : a/R = 0.04, 0.12, 0.24, 0.40, 0.60, 0.85.

Since there are 4 shapes ($\alpha=0$, 1/3, 2/3, 1) for each crack depth, 24 geometries are analyzed in all.

Loads. Three loads are applied on the cracks :

. a uniform pressure σ, which corresponds to the bar under tension (Fig.2a),

. a linear pressure of maximal value σ, which corresponds to the bar bended along the axis perpendicular to the symmetry axis of the cracked section (Fig.2b),

. a shear stress distribution of maximal value τ, which corresponds to the bar under torsion (Fig.2c).

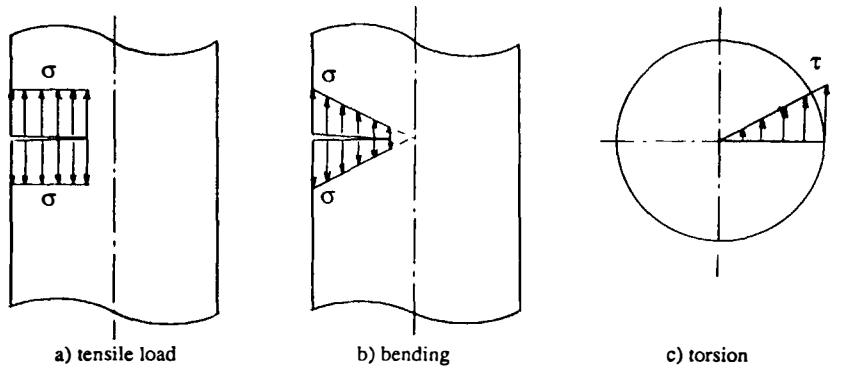

Fig. 2. Loads

COMPUTATIONS

The bar is assumed to be made of a linear elastic, isotropic, homogeneous material. To solve the problem, use has been made of the integral equation given by Levan et al. (1986) for three-dimensional cracks.Following this formulation, the lateral surface of the bar is considered as a fictitious crack crossing the actual one. The discretization of the integral equation has been performed by the finite element method and the mesh covers the circular crack together with the lateral surface of the bar. Of course, should the different loads be treated separately, then symmetries or skew-symmetries could have been exploited so that the problem is reduced to the study of one quarter of the bar, provided that adequate boundary conditions are added. This reduction is not carried out here for two reasons : first, the whole structure is preserved so that several loads could be applied simultaneously and one has to solve the algebraic system once only; secondly, the matrix of the system being fully populated and moreover non-symmetrical, as is the case with any integral equation method, the obtention of symmetrical or skew-symmetrical results ensures the accuracy of input data.

Eventually the nodal vector $\vec{\varphi}$ is obtained, as the density of the singular kernel of the above-mentioned integral equation. As shown by Kupradze (1963) and Bui (1977), this vector is exactly equal to the displacement discontinuity across the crack surface. From the nodal values, the complete vector field $\vec{\varphi}$ defined on the crack can be determined using classical shape functions. At every point on the crack front, one can then determine the stress intensity factors defined as :

$$
\begin{aligned}
K_I &= E/(8(1-\nu^2)) \lim_{\rho \to 0} \varphi_n/\sqrt{(2\pi/\rho)} \\
K_{II} &= E/(8(1-\nu^2)) \lim_{\rho \to 0} \varphi_v/\sqrt{(2\pi/\rho)} \qquad (1) \\
K_{III} &= E/(8(1+\nu)) \lim_{\rho \to 0} \varphi_t/\sqrt{(2\pi/\rho)}
\end{aligned}
$$

where E is the Young modulus, ρ denotes the distance to the tangent to the crack front; φ_n designates the normal out-of-plane component of φ, φ_v and φ_t are respectively the in-plane radial and tangential components of $\vec{\varphi}$ in the local basis at each point on the crack front.

NUMERICAL RESULTS

For all numerical purposes, the Poisson ratio ν is taken to be equal to 0.3.
By means of relation (1), the stress intensity factors are computed at every nodes located on the crack front. For each crack geometry, i.e. for each couple of values (a/R, α), one obtains 4 *discrete* curves for the following normalized stress intensity factors :

. $K_I/\sigma\sqrt{(\pi a)}$ for the bar under tensile loading,
. $K_I/\sigma\sqrt{(\pi a)}$ for the bar under bending, (2)
. $K_{II}/\tau\sqrt{(\pi a)}$ and $K_{III}/\tau\sqrt{(\pi a)}$ for the bar under torsion.

These factors are functions of the relative abcissa s/s_0 where s denotes the curvilinear abcissa on the front, with origin at the deepest point of the crack (point A in Fig.1a), oriented from A to B; while s_0 denotes the half-length of the crack front (the length of arc AB in Fig.1a).
Fig.3 shows the 4 curves of normalized stress intensity factors versus s/s_0 for the geometry (a/R=0.4, α=1).

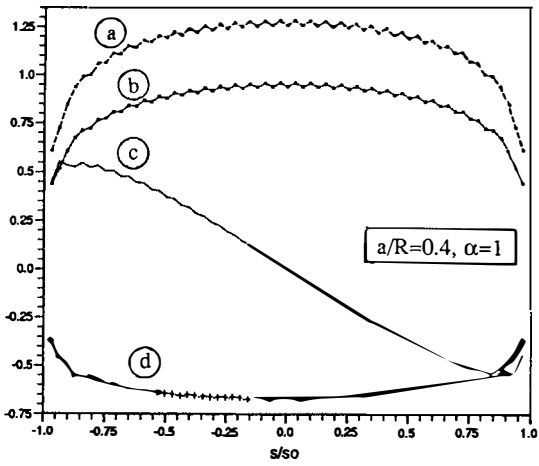

Fig. 3. Normalized stress intensity factors versus s/s_o

ⓐ : $K_I/\sigma\sqrt{(\pi a)}$, tension:
ⓑ : $K_I/\sigma\sqrt{(\pi a)}$, bending
ⓒ : $K_{II}/\tau\sqrt{(\pi a)}$ } torsion
ⓓ : $K_{III}/\tau\sqrt{(\pi a)}$ }

Using the least square method, the set of discrete values of stress intensity factors obtained for 24 geometries under consideration has been fitted in the following expressions :

$$K_I/\sigma\sqrt{(\pi a)} = \sum_i \sum_j \sum_k c_{ijk} (a/R)^i \alpha^j (s/s_o)^k$$

$$K_{II}/\tau\sqrt{(\pi a)} = \sum_i \sum_j \sum_k c_{ijk} (a/R)^i \alpha^j (s/s_o)^k \qquad (3)$$

$$K_{III}/\tau\sqrt{(\pi a)} = \sum_i \sum_j \sum_k c_{ijk} (a/R)^i \alpha^j (s/s_o)^k$$

Four sets of coeffients c_{ijk} are then obtained for 4 types of stress intensity factors in relation (2).

Stress Intensity Factor Variation along the Crack Front. Fig.4 shows the variation of the normalized stress intensity factors versus the crack front, for the relative crack depth a/R= 0.4. It may be seen from Fig.4a that, in the case of a uniform pressure applied on the crack, the curvature of the K_I curve changes in sign when passing from the semi-circular crack to the straight-fronted one. According to the crack shape, the maximum of K_I is either at the deepest point of the crack or at a point near the surface terminal point. This is clearly shown on the perspective view of the K_I surface versus α and s/s_o (Fig.5) : when s/s_o tends to ± 1, K_I either increases or decreases according to the value of α. A crack shape can be observed, in this case when α is approximately equal to 1/3, such that K_I remains virtually constant along the crack front. This means that if the iso-K_I criterion is chosen in order to predict the propagation of cracks created by mode I fatigue, the actual crack shape is that which corresponds to $\alpha = 1/3$.

Likewise, Fig.4b shows that the crack takes the shape corresponding to $\alpha = 2/3$ under a linear pressure.

Figs.4c and 4d show the stress intensity factors K_{II} and K_{III} arising from a torque applied at the ends of the bar. It should be noticed that K_{II} varies almost as a linear function of the curvilinear abcissa. On the other hand, for all crack shapes, K_{III} is, in absolute values, maximal at the deepest point. In any case, the aspect of K_{II} and K_{III} curves are little influenced by the crack shape, contrary to what happens to K_I curves.

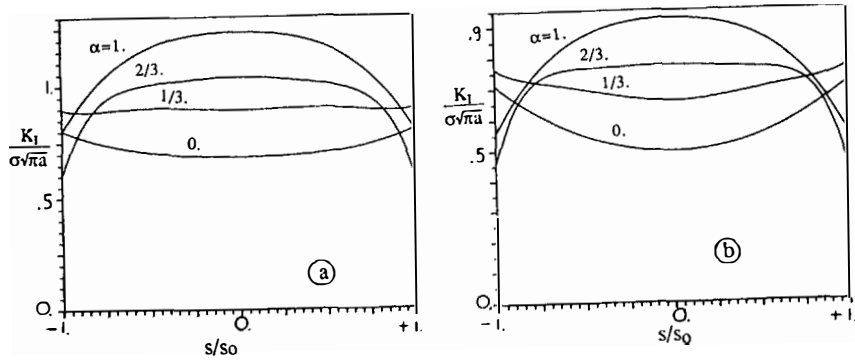

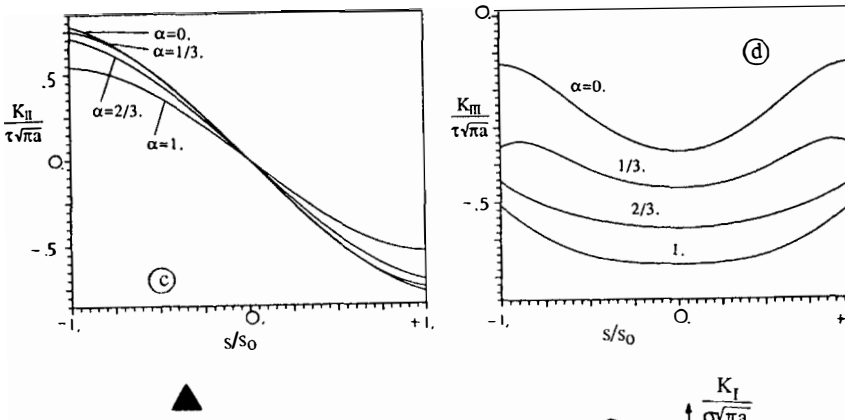

Fig. 4. Variation of normalized stress intensity factors along the crack front for a/R=0.4
a) K_I in tension
b) K_I in bending
c) K_{II} in torsion
d) K_{III} in torsion

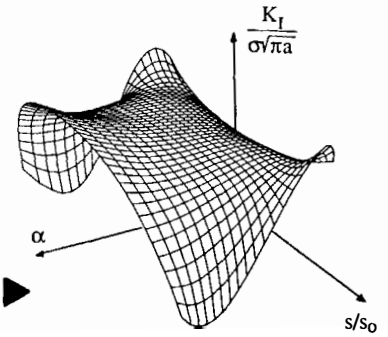

Fig. 5. Variation of stress intensity factor K_I as a function of crack front abcissa s/s_0 and crack shape α in a round bar under tension

It is also of importance to note that the stress intensity factors values are valid only over about 80% of the crack front length. The values for s/s_0 approaching ± 1 are affected by phenomena extraneous to the present work, such as the vicinity of the surface terminal points B or B' (see Fig.1a) that modifies the crack tip singularity. Also, the distortion of the finite element mesh around these zones must lower the accuracy of the numerical results. Anyway, the results obtained by Bazant et al. (1979) prove that the crack tip singularity at the surface point depends on the Poisson ratio ν and the terminal point incident angle θ (see Fig.1a) between the crack front and the surface line BB'. For a given value of ν, there exists a limiting value of θ for which the stress intensity factor K_I tends to a non zero finite value. If θ is less than this limit value, K_I falls off to zero and if θ is greater, K_I becomes infinite. In both cases K_I classically defined loses its physical meaning.

Stress Intensity Factor Variation versus the Crack Depth. Fig. 6 shows normalized K_I, K_{III} at the deepest point (s=0) resulted from the basic loads, tension, bending and torsion, and their dependance on the relative crack depth a/R. Factor K_{II} is not plotted since it is identically zero at s=0. For one load there are four K_I or K_{III} curves which relates individually to one crack shape, α=0, 1/3, 2/3, or 1. In Fig.6a, the lower curve relates to the semi-circular crack (α=0) and the upper to the straight-fronted crack (α=1). These two curves show that normalized K_I increases with a, whereas the other two (α=1/3 and 2/3) indicate that factor K_I, which certainly increases with a, may decrease when normalized by $\sigma\sqrt{(\pi a)}$.

The limit value of K_I for straight-fronted cracks when a/R tends to zero is, either in the case of tensile loading or bending, 1.128, which compares well with the theoretical value 1.122 for the edge crack in the semi-infinite body (Koiter, 1965). On the other hand, the same limit value of K_I for semi-circular cracks is 0.686, which is about 8% above the theoretical value $2/\pi$=0.6366 for the penny-shaped crack embedded in the infinite body. This difference can be compared to the limit values obtained by Raju et al. (1979), ≈0.668, that amounts to 5% above the same theoretical value, by Hayashi et al. (1980) (≈0.69, 8%), and by Astiz (1986a) (0.738, 16%). The rise of the K_I value can be easily accounted for by the presence of the free lateral surface of the bar that allows a wider crack opening, thus a greater K_I.

It should be noticed that the slopes at a/R=0 of the K_I curves for semi-circular and straight-fronted cracks is zero in the case of tensile loading, as it can be predicted theoretically. In the case of bending, these slopes are of the same order than the theoretical ones, respectively -23° and -34°3.

In Fig.7, the present results for K_I in the case of tensioned bars containing semi-circular or straight-fronted cracks are compared to those of Astiz (1986a), Caspers et al. (1987) and Raju et al. (1984), related to semi-elliptical cracks which admit of the same limit crack shapes.

CONCLUSION

Surface circular cracks in a round bar have been investigated, providing either K_I, K_{II} or K_{III} values. The analysis also includes the variation of these stress intensity factors along the crack front. Fittings of the numerical results by means of simple polynomials then make possible the calculation of any crack geometry of this type under combined loads, with an expected accuracy of 1%.

The knowledge of mixed mode stress intensity factors at every point of the crack front must allow to predict the mechanical behaviour of circular cracks in a round bar subject to various loads. The present method can easily be applied to pipes containing through or part-through cracks, it can also be used to predict the shape of cracks propagated in mode I, according to Poisson's ratio ν.

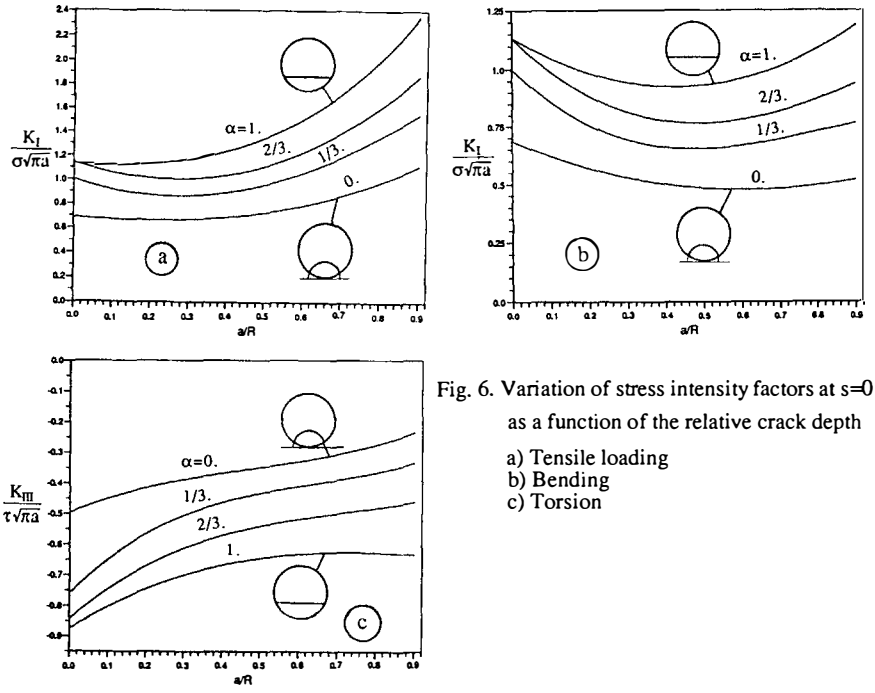

Fig. 6. Variation of stress intensity factors at s=0 as a function of the relative crack depth

a) Tensile loading
b) Bending
c) Torsion

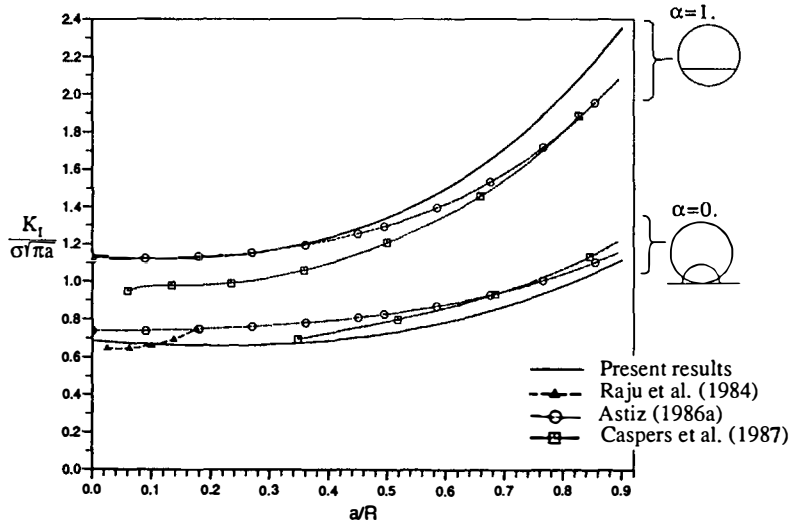

Fig. 7. Comparison of normalized stress intensity factors versus relative crack depth for semi-circular and straight-fronted cracks in a bar under tension

REFERENCES

M. A. Astiz, M. Elices (1980) - On the application of the stiffness derivative method to two and three dimensional fracture problems, Proceedings of the Second International Conference on Numerical Methods in Fracture Mechanics, Pineridge Press, Swansea, pp. 93-106
M. Astiz, M. Elices, J. Morton, A. Valiente (1981) - A photoelastic determination of stress intensity factors for an edge-cracked rod in tension, Proceedings of the Society for Experimental Stress Analysis, Spring Meeting, Dearborn, Michigan, pp. 277-282
M. A. Astiz (1986) - An incompatible singular elastic element for two- and three-dimensional crack problems, Int. J. Fract., pp. 105-124
M. A. Astiz, M. Elices, A. Valiente (1986) - Numerical and experimental analysis of cracked cylindrical bars, European Congress on Fracture, pp. 65-74
A. Athanassiadis, J. M. Boissenot, P. Brevet, D. François, A. Raharinaivo (1981) - Linear elastic fracture mechanics computations of cracked cylindrical tensioned bodies, Int. J.Fract., vol. 17, no 6, pp. 553-566
Z. P. Bazant, L. F. Estenssoro (1979) - Surface singularity and crack propagation, Int.J. Sol. and Struct., vol.15, pp. 405-426
W.S. Blackburn (1976) - Calculation of stress intensity factors for straight cracks in grooved and ungrooved shafts, Eng. Fract. Mech. vol.8, pp. 731-736
H.D. Bui (1977) - An integral equations method for solving the problem of a plane crack of arbitrary shape, J. Mech. Phys. Solids, vol. 25, pp. 29-39
A. J. Bush (1976) - Experimentally determined stress intensity factors for single-edge-crack round bars loaded in bending, Proceedings of the Society for Experimental Stress Analysis, vol. 33, no 2, pp. 249-257
M. Caspers, C. Mattheck (1987) - Weighted averaged stress intensity factors of circular-fronted cracks in cylindical bars, Fatigue Fract. Eng. Materials Structures, vol. 9, no 5, pp. 329-341
O. E. K. Daoud, D. J. Cartwright, M. Carney (1978) - Strain-energy release rate for a single-edge-cracked circular bar in tension, J. of Strain Analysis, Vol. 13, no 2, pp. 83-89
O. E. K. Daoud, D. J. Cartwright (1984) - Strain energy release rates for a straight-fronted edge crack in a circular bar subject to bending, Eng. Fract. Mech., vol. 19, no 4, pp. 701-707
Y-X. Fan, T-Y. Fan, D-J. Fan (1982) - The approximate analytical solution for both surface and embedded cracks in cylinder with finite size, Eng. Fract. Mech., vol. 16, no 1, pp. 55-67
R. G. Forman, V. Shivakumar (1984) - Growth behaviour of surface cracks in the circumferential plane of solid and hollow cylinders, In Fracture Mechanics, vol. 17, ASTM STP 905, 17th National Symposium on Fracture Mechanics, Albany, New York, pp. 59-74
K. Hayashi, H. Abé (1980) - Stress intensity factors for a semi-elliptical crack in the surface of a semi-infinite solid, Int. J. Fract., vol. 16, no 3, pp. 275-285
W. T. Koiter (1965) - Discussion on rectangular tensile sheet with symmeric edge cracks, J. Appl. Mech., vol. 23, p. 237
V. D. Kupradze (1963) - Dynamical problems in Elasticity. In Progress in Solid Mechanics, ed. by I.N. Sneddon and R. Hill, vol. III, North-Holland, Amsterdam
A. Levan, J. Royer (1986) - Integral equation for three-dimensional problems, Int.J. Fract., vol.31, pp. 125-142
K. Nezu, S. Machida, H. Nakamura (1982) - Stress intensity factor of surface cracks and fatigue crack propagation behaviour in a cylindrical bar, the 25th Japan Congress on Material Research, Metallic Metals, pp. 87-92
I.S. Raju, J. C. Newman (1979) - Stress intensity factors for a wide range of semi-elliptical surface cracks in finite thickness plates, Eng. Fract. Mech., vol. 11, no 4, pp. 817-829
I. S. Raju, J. C. Newman (1984) - Stress intensity factors for circumferential surface cracks in pipes and rods under tension and bending loads, In Fracture Mechanics, vol. 17, ASTM STP 905, 17th National Symposium on Fracture Mechanics, Albany, New York, pp. 789-805
A. S. Salah el din, J. M. Lovegrove (1981) - Stress intensity factors for fatigue cracking of round bars, Int. J. of Fatigue, vol. 3, pp. 117-123
J. H. Underwood, R. L. Woodward (1989) - Wide range stress intensity factor expression for an edge-cracked round bar bend specimen, Experimental Mechanics, vol. 29, no 2, pp. 166-168